

Element-specific recoil loops in Sm–Co/Fe exchange-spring magnets

Y. Choi,^{a)} J. S. Jiang, J. E. Pearson, and S. D. Bader
Materials Science Division, Argonne National Laboratory, Argonne, Illinois 60439, USA

J. P. Liu
Department of Physics, University of Texas at Arlington, Arlington, Texas 76019, USA

(Presented on 7 November 2007; received 9 September 2007; accepted 10 October 2007; published online 11 February 2008)

In two-phase nanocomposite magnets, open recoil loops have shown to be sensitive to interphase interfacial conditions and have been often used to characterize the interphase exchange coupling. Typically, the open recoil loops are attributed to the soft phase volume that is decoupled from the hard phase. Our element-specific magnetic measurements on bilayer Sm–Co/Fe exchange-spring magnets reveal that open recoil loops are present not only in the soft Fe layer but also in the hard Sm–Co layer and that the Fe- and Sm-specific remanence curves are similar to each other. The experimental results and micromagnetic modeling reveal that the observed open recoil loops can originate from the anisotropy variations in the hard Sm–Co layer. © 2008 American Institute of Physics. [DOI: 10.1063/1.2830231]

Based on the beneficial combination of the high magnetic anisotropy of a magnetically hard phase and the high saturation moment of a magnetically soft phase, exchange-coupled nanocomposite permanent magnets can have magnetic properties that are superior to those of single-phase magnets.^{1,2} In the nanocomposite magnets, the exchange coupling (with optimal exchange coupling length of a few nanometers) between the two phases is the principal mechanism of their enhanced maximum energy product values.¹ Thus, a better understanding of the exchange coupling is crucial in the development of nanocomposite magnets with improved magnetic properties.

Because of their observed sensitivity to interphase conditions, recoil loop measurements have been often used to characterize exchange-coupled nanocomposite permanent magnets, as demonstrated by previous studies.^{3–10} Recoil loops are measured by removing and reapplying a demagnetizing field to a magnetically saturated permanent magnet, as the demagnetizing field magnitude is increased successively [an example of the applied field history is shown in Fig. 1(c)]. When the magnetizing and demagnetizing branches do not overlap, the two branches enclose an area, forming an open recoil loop. Since open recoil loops are typically absent in single-phase magnets, the presence of open recoil loops is seen as a manifestation of decoupling between the soft and hard phases and the enclosed area is attributed to the decoupled volume in the soft phase.^{5–10}

We examine the possible origin of open recoil loops in exchange-spring magnets. Using element-resolved x-ray resonant magnetic scattering (XRMS) magnetometry,¹¹ we studied recoil loops from each layer separately in Sm–Co/Fe exchange-spring magnet films.^{1,2} Our experimental and simulation results show that the onset of the open recoil loops is not necessarily a direct consequence of the

decoupling between the two phases but rather originates from variations in the Sm–Co layer anisotropy.¹²

Two epitaxial Sm–Co/Fe exchange-spring bilayer samples with in-plane uniaxial anisotropy were fabricated using magnetron sputtering as described in Ref. 13. The Fe layer was deposited at 100 °C for one sample. For the other sample, the Fe layer was deposited at 400 °C in order to increase interdiffusion at the Sm–Co/Fe interface.¹³ These two samples are designated as T100 and T400, respectively, throughout this article.

Magnetic characterization results via vibrating sample magnetometry are shown in Fig. 1. The major demagnetizing curves show that the nucleation field is increased and the irreversible switching field is decreased for T400, in comparison with T100. The apparent increase in the coupling between the two layers is attributed to a graded interface effect.¹⁴ The recoil measurements show open areas enclosed by the demagnetizing and recoil curves, indicating the pres-

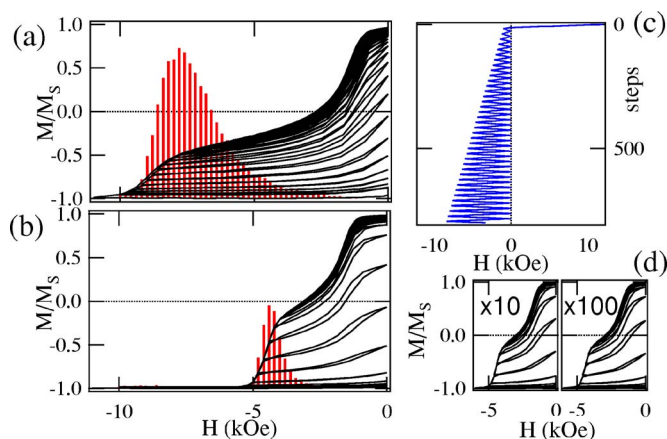


FIG. 1. (Color online) Easy axis recoil loops measured at 300 K for (a) T100 and (b) T400. Vertical bars represent recoil loop areas. (c) Applied field history. (d) T400 recoil measurements with increased measurement time.

^{a)}Also at the Department of Physics, University of Texas at Arlington, Arlington, TX 76019. Electronic mail: yschoi@anl.gov.

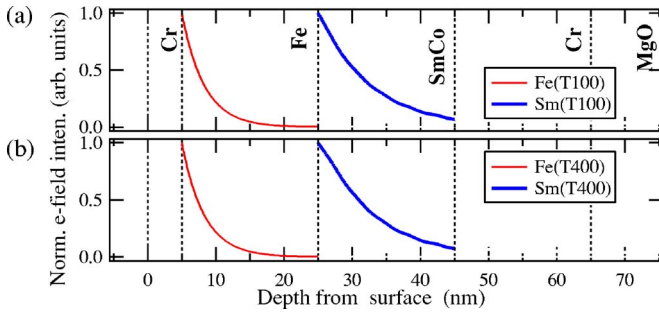


FIG. 2. (Color online) Calculated normalized electric field intensity profiles for (a) T100 and (b) T400. The calculations take into account the Sm–Co/Fe interfacial intermixing of 1 or 3 nm, respectively. These values cause only minimal differences between (a) and (b).

ence of irreversible processes during the recoil measurements. Differences in the overall trend of the open recoil loop areas are observable. To prove that the open recoil loops are not due to time-dependent magnetization decay, measurement time is increased by a factor of 10 or 100. As shown in Fig. 1(d), the measured recoil loops are nearly identical to Fig. 1(b).

The XRMS measurements were performed at beamline 4ID-C of the Advanced Photon Source at Argonne National Laboratory.¹⁵ The XRMS measurements were made at the Fe L_3 and Sm M_4 absorption edges to probe the Fe and Sm–Co layers, respectively. Element-specific recoil magnetization hysteresis loops were obtained at 200 K as a function of external magnetic field H at a fixed x-ray energy and specular angle. To estimate the probing depth in our XRMS measurements, we calculated an electric field intensity profile inside the film layers for each measurement,^{13,16} as shown in Fig. 2. The calculation results suggest that most of the measured Fe- and Sm-XRMS signals are from the top portions of the Fe and Sm–Co layers, respectively.

The element-specific recoil loops from the two samples are shown in Fig. 3. Both Fe and Sm recoil curves are completely reversible until the magnitude of the applied demagnetizing field is high enough to initiate reversal in the Sm–Co layer. Enclosed areas appear concurrently in both Fe and Sm recoil loops. The areas enclosed by a recoil loop persist until the demagnetizing field is much greater than the coercive field of the Sm major loop. Open recoil loops, measured by bulk magnetometry, as in Fig. 1, are often attributed to decoupled soft phase.^{5–8} In contrast, our element-specific measurements show that the open recoil loops are present not only in the soft (Fe) layer but also in the hard (Sm–Co) layer in our two samples that have different interface morphologies and extents of exchange coupling. As shown in Fig. 2, the Fe volume responsible for the measured Fe-XRMS recoil loops is spatially separated from the Sm–Co volume responsible for the Sm-XRMS recoil loops. If the decoupling were associated with open recoil loops, the top region of the Fe layer, which contributes most to the XRMS curves while being the farthest from the Sm–Co/Fe interface, would be the first region to become decoupled and reversible again. These results suggest that the presence of the open recoil loops may not be a consequence of the interphase decoupling.

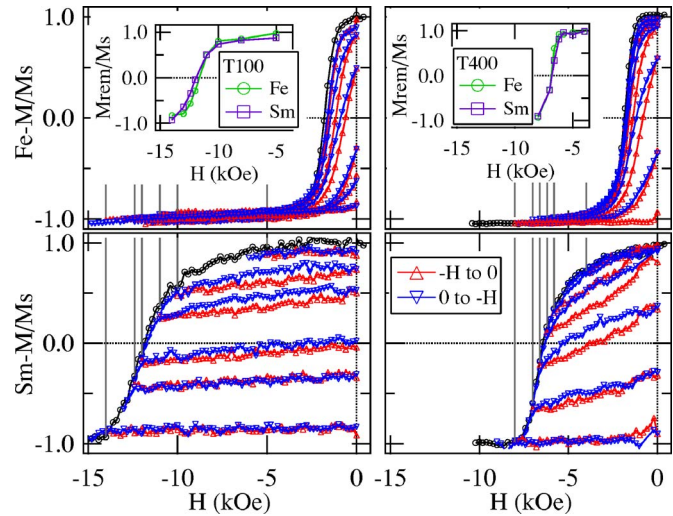


FIG. 3. (Color online) Element-specific recoil loops from T100 and T400 at 200 K. The dotted vertical lines indicate the initial field for each recoil curve. The major demagnetization curves (with circle symbol) are shown as a reference. Normalized remanence curves from the Fe and Sm recoil curves are shown as insets. Different triangle symbols represent different directions of the field sweep.

As shown in Fig. 3, the Fe layer becomes irreversible and open recoil loops appear for both layers only after the demagnetizing field is high enough to initiate magnetization reversal in the Sm–Co layer. This indicates that the open recoil loops may be related to lateral domain formation in the Sm–Co layer. In Fig. 3, normalized remanence curves from the element-specific recoil loops are shown as insets. For each sample, the Fe remanence curve mimics its Sm counterpart. The similarity between the Fe and Sm remanence curves in Fig. 3 suggests that, at $H=0$, the Fe layer mirrors the domain configuration in the Sm–Co layer below with the same area fraction of the reversed domains. Similar behaviors have been observed in SmFe/NiFe exchange-spring films where the soft and hard layers undergo lateral domain nucleation and growth along the demagnetizing and recoiling curves.¹⁷ One of the possible origins of this type of partial reversal is anisotropy variations in the hard layer. A previous study using high-resolution electron microscopy had shown that similarly grown nominally Sm₂Co₇ films contained regions with softer Sm–Co phases induced by stacking disorder along the c axis.¹⁸ There may be some weak Sm–Co grains with different anisotropy values in our films as well. Consistent with our current analysis, it has been reported that coercivity distribution and the volume fraction of the constituent phases are related to the origin of open recoil loops.¹⁹

To test whether the hard layer domains due to a distribution in hard layer anisotropy would give rise to the kind of hysteretic recoil behavior observed in our XRMS measurements, we simulated recoil measurements on the same Sm–Co/Fe bilayer structure using micromagnetic calculations.²⁰ Figure 4(a) shows the model Sm–Co/Fe structure for our simulations. The simulated volume is $L_x \times L_y \times L_z = 300 \times 300 \times 40$ nm³ with periodic conditions in the x and y directions. The simulation cell size was $1 \times 300 \times 1$ nm³. The model includes three weak Sm–Co grains with

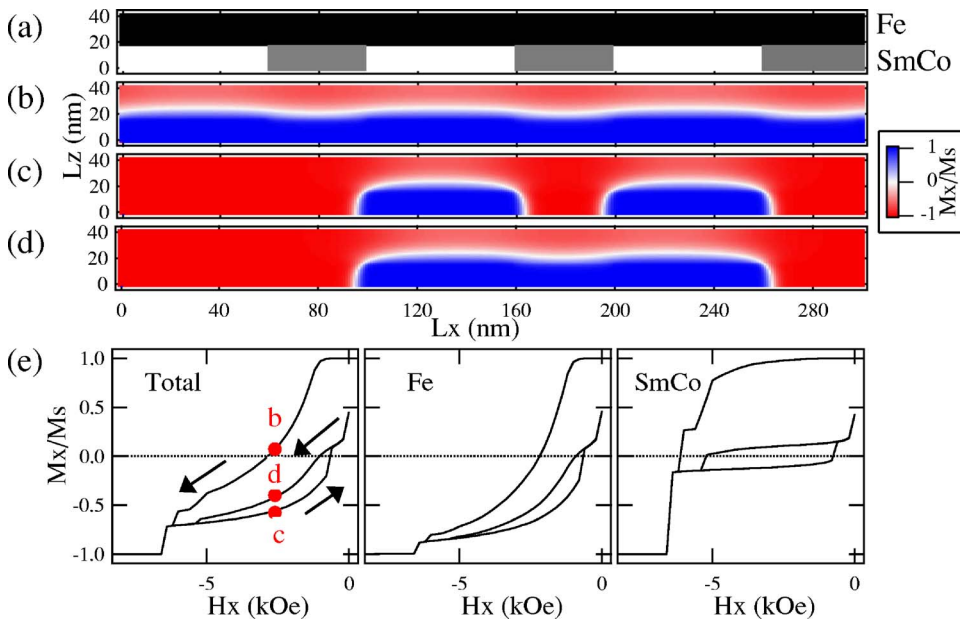


FIG. 4. (Color online) (a) A model Sm-Co/Fe structure containing three weak Sm-Co grains marked in gray. [(b)–(d)] Simulated magnetic configurations at different points but with the same field magnitude as indicated in (e). (e) Simulated recoil loops for the total, Fe, and Sm-Co layers. The arrows indicate the directions of the field sweep.

their anisotropy values reduced to 20%–22% of their nominal value. Other parameters are fixed using the parameters from Ref. 21. In this simulation model, there is no weakening of the exchange coupling between the Fe and Sm-Co layers or between the normal and weak Sm-Co grains.

In Fig. 4(e), the total and the individual Fe and Sm-Co layer contributions are plotted separately. Consistent with our XRMS experimental results, the open recoil loops are present in both layers with the same remanence values for both layers. As the demagnetizing field H increases, the Fe layer reverses its magnetization first [Fig. 4(b)]. Magnetization reversal initiates in the Sm-Co grains with the reduced anisotropy values [Fig. 4(c)]. As H is reduced back to zero, portions of the Fe layer and the weak Sm-Co grains reverse back to the original direction. The Fe and Sm-Co remanence values are reduced, as observed experimentally. An irreversible change occurs as the lateral domain walls collapse together along with the Fe region above, as shown in Fig. 4(d). As a result of the different demagnetizing and recoil paths, the recoil loop becomes open for the Fe and Sm-Co layers. In real samples with a much larger number of grains and with anisotropy distributions, this type of domain wall collapsing would occur continuously during a recoil measurement, contributing to multiple open recoil loops as seen in Figs. 1 and 3. While our model reproduced the open recoil loops, other simulation models with the interphase exchange coupling as a variable did not lead to open recoil loops.

Our combined approach of element-sensitive magnetic characterization and micromagnetic simulation sheds light on the origin of open recoil loops in exchange-coupled nanocomposite magnets. Our result indicates that the open recoil loops are linked to variations in the hard layer anisotropy rather than to interlayer decoupling. While the domain formation in the hard layer can also be considered as a consequence of the decoupling among hard layer grains, this is inherently different from the interlayer decoupling. Thus it is important to recognize that routine open recoil loop measurements on nanocomposite magnets do not provide straightfor-

ward information about the extent of interphase exchange coupling.

This work is supported by ONR/MURI under Grant No. N00014-05-1-0497 and by U.S. Department of Energy, Office of Science, under Contract No. DE-AC02-06CH11357.

- ¹E. F. Kneller and R. Hawig, IEEE Trans. Magn. **27**, 3588 (1991).
- ²R. Skomski and J. M. D. Coey, Phys. Rev. B **48**, 15812 (1993).
- ³M. Emura, D. R. Cornejo, and F. P. Missell, J. Appl. Phys. **87**, 1387 (2000).
- ⁴E. H. Feutrill, P. G. McCormick, and R. Street, J. Phys. D **29**, 2320 (1996).
- ⁵D. Goll, M. Seeger, and H. Kronmüller, J. Magn. Magn. Mater. **185**, 49 (1998).
- ⁶D. C. Crew, J. Kim, L. H. Lewis, and K. Barmak, J. Magn. Magn. Mater. **233**, 257 (2001).
- ⁷C. L. Harland, L. H. Lewis, Z. Chen, and B.-M. Ma, J. Magn. Magn. Mater. **271**, 53 (2004).
- ⁸K. Kang, L. H. Lewis, J. S. Jiang, and S. D. Bader, J. Appl. Phys. **98**, 113906 (2005).
- ⁹A. Bollero, O. Gutfleisch, K.-H. Müller, L. Schultz, and G. Drazic, J. Appl. Phys. **91**, 8159 (2002).
- ¹⁰J. Zhang, Y. K. Takahashi, R. Gopalan, and K. Hono, Appl. Phys. Lett. **86**, 122509 (2005).
- ¹¹J. W. Freeland, K. Bussmann, P. Lubitz, Y. U. Idzerda, and C.-C. Kao, Appl. Phys. Lett. **73**, 2206 (1998).
- ¹²Y. Choi, J. S. Jiang, J. E. Pearson, S. D. Bader, and J. P. Liu, Appl. Phys. Lett. **91**, 022502 (2007).
- ¹³Y. Choi, J. S. Jiang, Y. Ding, R. A. Rosenberg, J. E. Pearson, S. D. Bader, A. Zambano, M. Murakami, I. Takeuchi, Z. L. Wang, and J. P. Liu, Phys. Rev. B **75**, 104432 (2007).
- ¹⁴J. S. Jiang, J. E. Pearson, Z. Y. Liu, B. Kabius, S. Trasobares, D. J. Miller, S. D. Bader, D. R. Lee, D. Haskel, G. Srajer, and J. P. Liu, Appl. Phys. Lett. **85**, 5293 (2004).
- ¹⁵J. W. Freeland, J. C. Lang, G. Srajer, R. Winarski, D. Shu, and D. M. Mills, Rev. Sci. Instrum. **73**, 1408 (2001).
- ¹⁶L. G. Parratt, Phys. Rev. **95**, 359 (1954).
- ¹⁷D. Chumakov, R. Schäfer, D. Elefant, D. Eckert, L. Schultz, S. S. Yan, and J. A. Barnard, Phys. Rev. B **66**, 134409 (2002).
- ¹⁸M. Benaissa, K. M. Krishnan, E. E. Fullerton, and J. S. Jiang, IEEE Trans. Magn. **34**, 1204 (1998).
- ¹⁹R. W. McCallum, J. Magn. Magn. Mater. **299**, 472 (2006).
- ²⁰Using the LLG micromagnetics simulator (<http://llgmicro.home.mindspring.com>).
- ²¹E. E. Fullerton, J. S. Jiang, M. Grimsditch, C. H. Sowers, and S. D. Bader, Phys. Rev. B **58**, 12193 (1998).